A geometrical approach to *SU*(2) navigation with Fibonacci anyons

2008 J. Phys. A: Math. Theor. 41 175302

(http://iopscience.iop.org/1751-8121/41/17/175302)

IOP PUBLISHING JOURNAL OF PHYSICS A: MATHEMATICAL AND THEORETICAL

J. Phys. A: Math. Theor. **41** (2008) 175302 (12pp) doi:10.1088/1751-8113/41/17/175302

A geometrical approach to $SU(2)$ navigation with Fibonacci anyons

Rémy Mosseri

Laboratoire de Physique Théorique de la Matière Condensée, CNRS UMR 7600, Université UPMC Paris, 4 Place Jussieu, 75252 Paris Cedex 05, France

E-mail: mosseri@ccr.jussieu.fr

Received 17 January 2008
Published 15 April 2008
Online at stacks.iop.org/JPhysA/41/175302

Abstract

Topological quantum computation with Fibonacci anyons relies on the possibility of efficiently generating unitary transformations upon pseudoparticles braiding. The crucial fact that such a set of braids has a dense image in the unitary operations space is well known; in addition, the Solovay–Kitaev algorithm allows us to approach a given unitary operation to any desired accuracy. In this paper, the latter task is fulfilled with an alternative method, in the $SU(2)$ case, based on a generalization of the geodesic dome construction to higher dimension.

PACS numbers: 05.30.Pr, 03.67.Lx, 03.65.Ld

(Some figures in this article are in colour only in the electronic version)

1. Introduction

Topological quantum computation (TQC) [1–4] makes use of the subtle properties of topological phases of matter to provide an original implementation for quantum computation, better immune to decoherence. Its main ingredients are anyonic excitations displaying non-Abelian braiding statistics. Although no direct experimental proof exists that such characteristics occur in real physical systems, there is some evidence that, for instance, the $12/5$ fractional quantum Hall effect states should be good candidates to display the expected properties.

Up to now, contributions to the TQC field have mainly been split into two parts, a 'hardware' part whose main purpose is to find microscopic models and possible experimental realizations displaying these topological features in their spectral properties, and a 'software' part, which starts from a formal (non-Abelian) anyon model and defines, out of it, qubit states, quantum gates and algorithms. Note that this splitting is already present in more 'standard' quantum computation, with on one hand the large effort being devoted to building

experimental implementations of sets of coupled qubits, and the quantum algorithm part, which in fact started first, and most often does not discriminate between the very different microscopic realizations for the qubits, supposing that a large number of them are already available.

In the present paper, we analyze a model with three Fibonacci anyons (irrespective of their implementation), and ask how their manipulation (upon braiding) can appropriately approximate the action of generic $SU(2)$ unitary transformations. As is well known [2], this is in principle possible to any desired accuracy, thanks to the fact that the associated non-Abelian braid group representation is dense in $SU(2)$. To make this system interesting, it is also important that this can be done efficiently. Such a task has been fulfilled [5, 6] by splitting the braid search into two distinct parts: first, a brute force search among all braids up to a given length to generate the closest matrix to the target one; then, a refinement step done by iteratively implementing the Solovay–Kitaev algorithm [7, 8]. With additional Fibonacci anyons, it is possible to define more qubits, whose interaction results from an appropriate braiding. For example, a universal set of quantum gates has been derived [5, 6], with six anyons forming a two-qubit system, proving that it can in principle allow for quantum computation.

Here an alternative approach is proposed, of rather a different nature, in order to generate the $SU(2)$ elements. Instead of first insisting on the dense $SU(2)$ covering generated by the Fibonacci braid group generators, we start by analyzing how good the latter can approximate the generators of binary polyhedral $SU(2)$ finite subgroups. It comes out that the subgroup of higher order, the binary icosahedral group Y with 120 elements, can indeed be very efficiently approached. Recalling the isomorphism between $SU(2)$ and the three-dimensional sphere S^3, this already allows a fine grained description of $SU(2)$. Indeed, to the group Y corresponds the regular polytope $\{3, 3, 5\}$ [9, 10], whose full symmetry group G (discrete subgroup of $O(4)$) has order 14 400. This already leads to an efficient way of generating 14 400 $SU(2)$ unitary transformations, related by symmetry.

We further show how to iteratively get finer and finer meshes in $SU(2)$ by generating the so-called geodesic hyperdomes, the analogous with one dimension more, of the celebrated families of geodesic domes which provide fine discrete approximations of the usual sphere S^2.

In the final part, a more 'disordered' version of the latter step is described, which already provides an efficient speedup for 'brute-like' search.

2. Binary icosahedral group generation with Fibonacci anyons

Fibonacci anyons are quasiparticles displaying non-Abelian statistics upon braiding. We will not recall here the whole derivation of their properties, which can be found elsewhere [2–6], but only summarize what is used in the present context. What we need here is an expression for the two generators of the associated (non-Abelian) two-dimensional representation of the braid group B_3. A close inspection of the braiding and fusion rules, taking into account the need to satisfy the so-called pentagon and hexagon equations, allows us to find a set of generators.

As shown in [2], a qubit (2-level) system can be associated with three Fibonacci anyons, with a third state (called 'non-computational') which is not coupled to the first two upon anyons braiding. We shall therefore focus on the $SU(2)$ unitary action (up to a global phase) onto the qubit space.

2.1. Braid group generators for Fibonacci anyons

Generally speaking, a representation of the braid group B_n has $n-1$ generators σ_j satisfying the following two simple relations,

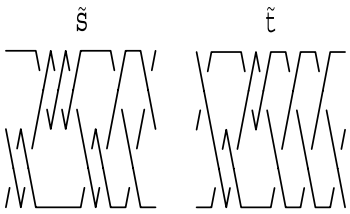

Figure 1. Graphical representation for the pseudo-generator braids $\tilde{s}$ and $\tilde{t}$, built as words in the σ_1 and σ_2 Fibonacci generators. Note that σ_1 (resp. σ_2) refers to crossing the upper (resp. the middle) braid with the middle (resp. the lower) braid, with the convention that the upper braid crosses 'on top' of the lower braid (the reverse case coding the inverse σ_1^{-1} and σ_2^{-1}).

$$\begin{aligned} &\sigma_i\sigma_j = \sigma_j\sigma_i, && |i-j| \geqslant 2 \\ &\sigma_j\sigma_{j+1}\sigma_j = \sigma_{j+1}\sigma_j\sigma_{j+1}, && 1 \leqslant j \leqslant n-2, \end{aligned} \tag{1}$$

which already limit the set of possible σ_j matrices. Fibonacci fusion rules constrain further this set, which eventually leads to the following unique (up to a phase) solution in the B_3 case:

$$\sigma_1 = \begin{pmatrix} \exp(-7\mathrm{i}\pi/10) & 0 \\ 0 & \exp(7\mathrm{i}\pi/10) \end{pmatrix}, \tag{2}$$

$$\sigma_2 = \begin{pmatrix} -\tau\exp(-\mathrm{i}\pi/10) & -\mathrm{i}\sqrt{\tau} \\ -\mathrm{i}\sqrt{\tau} & -\tau\exp(\mathrm{i}\pi/10) \end{pmatrix} \tag{3}$$

with $\tau = (\sqrt{5}-1)/2$ the inverse golden mean. Note that σ_1 and σ_2 both satisfy

$$\sigma_1^{10} = \sigma_2^{10} = -1. \tag{4}$$

Now, any braid is represented as a product of the σ_j generators. It also allows for an unambigous graphical presentation, where σ_j is displayed as a crossing between the braid lines j and $j+1$ (see, for example, figure 1). A word of caution should be given here concerning the braid ordering. Braid words are literally given and drawn here, as usual, with time flowing from left to right. Quantum qubit states, however, are represented as column vectors acted on the left by unitary matrices. Therefore, to build the unitary matrix corresponding to a braid word requires us to reverse the order from the braid word to the associated matrix product.

2.2. Binary polyhedral groups: geometry and generators

Due to the 2:1 homomorphism between $SU(2)$ and $SO(3)$, discrete $SU(2)$ subgroups have a counterpart as point groups in R^3. Let us focus here on the binary tetrahedral T (order 24), octahedral O (order 48) and icosahedral Y (order 120) groups. When viewed as elements of S^3, T and Y correspond to the regular polytopes $\{3,4,3\}$ and $\{3,3,5\}$ [9, 10]. The group presentations are given here together with sets of simple quaternion generators (see appendix A for a brief presentation of quaternions).

- Binary tetrahedral group T

$$\begin{aligned} &\langle s,t|s^3 = t^3 = (st)^2 = -1\rangle \\ &s = (1+i+j+k)/2 \\ &t = (1+i+j-k)/2 \end{aligned} \tag{5}$$

- Binary octahedral group O

$$\begin{aligned} &\langle s, t | s^3 = t^4 = (st)^2 = -1 \rangle \\ &s = (1 + i + j + k)/2 \\ &t = (1 + i)/\sqrt{2} \end{aligned} \tag{6}$$

- Binary icosahedral group Y

$$\begin{aligned} &\langle s, t | s^3 = t^5 = (st)^2 = -1 \rangle \\ &s = (1 + i + j + k)/2 \\ &t = (\tau^{-1} + \tau i + j)/2. \end{aligned} \tag{7}$$

2.3. The binary icosahedral group approached with Fibonacci anyons

We recalled above that the braid group B_3 representation with Fibonacci anyons is dense in $SU(2)$. We now question the possibility of generating the binary icosahedral subgroup by imposing some constraints on the words generated with $\{\sigma_1, \sigma_2\}$. Trying to build new generators $\tilde{s}$ and $\tilde{t}$ from $\{\sigma_1, \sigma_2\}$, which would follow the above-recalled generating relations for Y, we eventually find that while two of the three relations are easily and exactly fulfilled, the third one seems to be only asymptotically satisfied with longer and longer words. We call these cases 'pseudo-generators'. A brute force search for best words up to length 10 already gives the following very good approximations:
a pseudo-generator $\tilde{s} = \sigma_2^2 \sigma_1^{-3} \sigma_2^2 \sigma_1^{-1} \sigma_2 \sigma_1$

$$\tilde{s} = \begin{pmatrix} 0.5 - 0.706\,298\mathrm{i} & -0.428\,519 - 0.259\,8349\mathrm{i} \\ 0.428\,519 - 0.259\,8349\mathrm{i} & 0.5 + 0.706\,298\mathrm{i} \end{pmatrix} \tag{8}$$

$$\text{with} \quad \tilde{s}^3 = \begin{pmatrix} -1 & 0 \\ 0 & -1 \end{pmatrix}$$

and a pseudo-generator $\tilde{t} = \sigma_1 \sigma_2^2 \sigma_1^{-2} \sigma_2 \sigma_1^{-1} \sigma_2 \sigma_1^{-1} \sigma_2$

$$\tilde{t} = \begin{pmatrix} -0.309\,017 + 0.159\,002\mathrm{i} & -0.414\,981 + 0.840\,843\mathrm{i} \\ 0.414\,981 + 0.840\,843\mathrm{i} & -0.309\,017 - 0.159\,002\mathrm{i} \end{pmatrix} \tag{9}$$

$$\text{with} \quad \tilde{t}^5 = \begin{pmatrix} -1 & 0 \\ 0 & -1 \end{pmatrix}.$$

These two pseudo-generators are shown in figure 1. Note that in the above two expressions, the numerical values are cut up to six or seven digits; but the $\tilde{s}$ and $\tilde{t}$ exact expressions, as products of the $\{\sigma_1, \sigma_2\}$ Fibonacci generators, are such that $\tilde{s}^3 = \tilde{t}^5 = -1$ is exact. Finally, the third binary icosahedral group generating relation is only almost fulfilled

$$(\tilde{s}\tilde{t})^2 = \begin{pmatrix} -0.999\,995 + 0.000\,529\mathrm{i} & -0.001\,483 - 0.002\,677\mathrm{i} \\ 0.001\,483 - 0.002\,677\mathrm{i} & -0.999\,995 - 0.000\,529\mathrm{i} \end{pmatrix}. \tag{10}$$

Now, it is easy to build, with short words in the pseudo-generators $\{\tilde{s}, \tilde{t}\}$, a set denoted by $\tilde{Y}$ corresponding to a very slightly deformed $\{3, 3, 5\}$ polytope. Since $\{\tilde{s}, \tilde{t}\}$ do not exactly fulfil the Y generating relations, their span is in principle infinite. What we are doing in fact is to select, once for all, 120 words in $\{\tilde{s}, \tilde{t}\}$ (e.g. 120 braids) which very closely approximate the Y elements. The word length never exceeds 8, which puts an upper bound of 80 to the length of the $\tilde{Y}$ elements in terms of the original $\{\sigma_1, \sigma_2\}$ Fibonacci generators.

Note that it may still be possible to find shorter words leading to a good approximation of Y, either by the process of word contraction or by finding equivalent approximations by

the brute force search in the original generators. We are not interested here in absolute length minimization, but rather in describing a fine grid mesh based on a discrete subgroup and a geodesic hyperdome iterative generation; we shall therefore stick to $\{\tilde{s}, \tilde{t}\}$ generated braids.

3. Iterative fine meshes in $SU(2)$ with geodesic hyperdomes

We are going to build increasing sets $\mathcal{P}_i$ and $\mathcal{Q}_i$ which are the images under the full G group of seed sets of points (denoted by $\mathcal{S}_i^{\mathcal{P}}$ and $\mathcal{S}_i^{\mathcal{Q}}$) inside the orthoscheme $\mathcal{O}$ (the G group fundamental region, see appendix C). The $\mathcal{P}_i$, having the form of 'geodesic hyperdomes', were introduced, more than 20 years ago, in the very different context of atomic structures with long-range icosahedral order [11, 12]. More precisely, those $\mathcal{P}_i$ all shared the exact G subgroup of $O(4)$, while here the sets $\mathcal{P}_i$ follows approximate symmetry operations $\tilde{G}$, built from $\tilde{Y}$. But from now on, we shall no longer differentiate between the exact Y and the approximate $\tilde{Y}$ in describing these sets. These polytopes $\mathcal{P}_i$ are built such that the vertices' local order is very close to that of the $\{3, 3, 5\}$ vertices. In particular they have (slightly deformed) tetrahedral cells, each of which being decomposed into 24 smaller tetrahedra, which divide the larger tetrahedron in a way similar to the exact orthoscheme division of a $\{3, 3, 5\}$ cell (see appendix D, and for more details, [11, 12]). The $\mathcal{Q}_i$ sets correspond to this finer division of the $\mathcal{P}_i$, with one generic point in each orthoscheme-like tetrahedron.

In order to generate, with Fibonacci anyons, the corresponding sets of unitary matrices, one proceeds as follows. To get the full 14 400 images (under G) of a generic matrix q (noted as a unit quaternion) one must generate the elements (see appendix C) lqr and $l\bar{q}r$ with $l, r \in Y$. In terms of braiding operations, l and r are, once for all, put into one-to-one correspondence with braids (also noted as l and r for convenience) written in the generators $\tilde{s}$ and $\tilde{t}$. The central braid associated with the (seed) matrix q is then concatenated on the left and the right by l and r.

3.1. The $\mathcal{P}_0$ and $\mathcal{Q}_0$ first meshes

The first case is very simple and directly associated with the binary icosahedral group Y. $\mathcal{P}_0$ corresponds to the $\{3, 3, 5\}$ polytope; the seed set $\mathcal{S}_0^{\mathcal{P}}$ is just an orthoscheme vertex corresponding to one element of Y. $\mathcal{Q}_0$ is the maximal set invariant under the full G group symmetry, and $\mathcal{S}_0^{\mathcal{Q}}$ contains one point inside the orthoscheme.

In order to represent the $SU(2)$ elements, we shall use a Hopf map from $SU(2)$ onto the complex plane, as explained in appendix B. Figure 2 (left) shows the Hopf maf of $\mathcal{P}_0$; the obtained orientation on S^3 is generic, which leads to a full Hopf map showing 60 distinct elements on the base space (a fibre containing only two opposite matrices $\pm M \in SU(2)$). Only 51 among these 60 base points are shown here on a limited region. With the full Hopf map (with an inverse stereographic projection onto S^2), this set of 60 points forms a semi-regular polyhedron with icosahedral symmetry. Figure 2 (right) displays the Hopf map of the $\mathcal{Q}_0$14 400 elements. Note that this set, although much denser, still has some uncovered regions (of pseudo-pentagonal shapes).

3.2. The finer meshes $\mathcal{P}_1$ and $\mathcal{Q}_1$

The set $\mathcal{P}_1$ corresponds to the first step of a geodesic hyperdome generation, as discussed in appendix D. It contains 2160 points on S^3, which are the images under G of $\mathcal{S}_1^{\mathcal{P}}$ made of three different points in the orthoscheme $\mathcal{O}$.

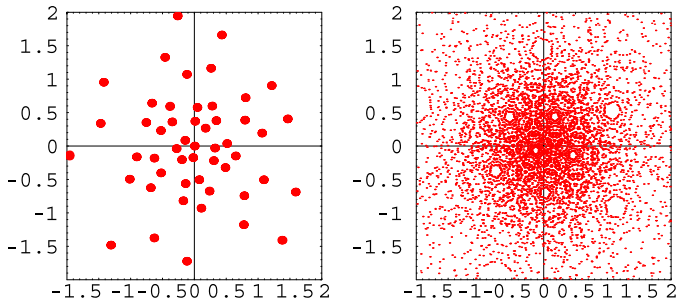

Figure 2. Hopf map (onto the complex plane) of sets of $SU(2)$ elements. Left: the set $\tilde{Y}$ (e.g. $\mathcal{P}_0$) with its 120 elements obtained from the pseudo-generators braids $\tilde{s}$ and $\tilde{t}$, which map onto 60 distinct points, one being sent to infinity and 51 being shown on this limited region. Right: Hopf map of the (14 400 elements) set $\mathcal{Q}_0$.

One point coincides with a {3, 3, 5} vertex (which is also an orthoscheme vertex), and can therefore be chosen conveniently as the identity matrix (in terms of braiding operation, this means no braid in the seed region). The other 119 images can simply be taken by applying Y either on the left or on the right.

The second seed point in $\mathcal{O}$ is also an orthosheme vertex, located at the centre of a {3, 3, 5} tetrahedral cell; the whole 600 images under G give a {5, 3, 3} polytope [9].

The third points sit along a {3, 3, 5} edge, at 1/3 of the total edge length from a vertex. There are 1440 such points.

So, in order to generate $\mathcal{S}_1^{\mathcal{P}}$, one only needs to generate two new $SU(2)$ matrices corresponding to these last two seed points. Approximating these two matrices with Fibonacci anyons is done by the brute force search; reasonably good approximations are found upon inspection of all braids (in the $\{\sigma_1, \sigma_2\}$ initial Fibonacci generators) of limited length. Note that since the full G group is subsequently acted, it is not necessary that the initial brute force search generates the seed points in the same G group fundamental region; this point already improves greatly the speed of that search step, and will be a main ingredient of the alternative approach presented in section 4.

The set $\mathcal{Q}_1$ is more complex to generate. $\mathcal{P}_1$ has 12 000 (almost regular) tetrahedral cells. Each such cell can be subdivided into 24 smaller tetrahedra, in a way similar to the division of the perfect tetrahedral $\mathcal{P}_0$ cells into 24 orthoscheme copies. As a whole $\mathcal{Q}_1$ has 288 000 elements. The corresponding set $\mathcal{S}_1^{\mathcal{Q}}$ contains 20 points. Here again, the associated 20 $SU(2)$ matrices are generated by the brute force search into finite length braids.

3.3. The set of iterative finer meshes $\mathcal{P}_i$ and $\mathcal{Q}_i$

The above construction of $\{\mathcal{P}_1, \mathcal{Q}_1\}$ from $\{\mathcal{P}_0, \mathcal{Q}_0\}$ can be iterated *ad infinitum*. It can be seen simply as a site decoration procedure; it can also be derived from a barycentric construction detailed in [12]. We do not intend to recall this method here and simply give in table 1 below some quantitative information. Note that the number of sites grows by a constant factor (20) at each step in the sets $\mathcal{Q}_i$.

4. An alternative method to $SU(2)$ discretization

The above iterative hyperdomes correspond to almost regular coverings of $SU(2)$. One can also proceed differently, and get, rather efficiently, less regular coverings. We know, from

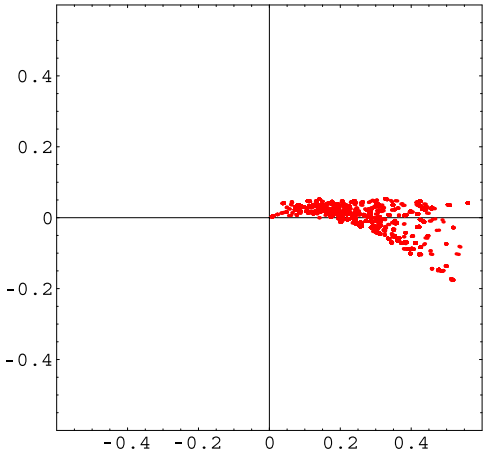

Figure 3. Hopf map (onto the complex plane) of $SU(2)$ matrices obtained from all words (up to length 7) in the $\{\sigma_1, \sigma_2\}$ Fibonacci generators, and brought back, modulo of the G group action, in the same orthoscheme $\mathcal{O}$.

Table 1. Number of sites ($SU(2)$ elements) in the first iterated hyperdomes $\mathcal{P}_i$ and related sets $\mathcal{Q}_i$.

$\mathcal{P}_0$	$\mathcal{Q}_0$	$\mathcal{P}_1$	$\mathcal{Q}_1$	$\mathcal{P}_2$	$\mathcal{Q}_2$	$\mathcal{P}_3$	$\mathcal{Q}_3$
120	14 400	2160	288 000	42 480	5760 000	847 440	115 200 000

the (once for all built) set $\tilde{Y}$, how to send any of the $14\,400G$ fundamental regions onto a given one $\mathcal{O}$; we can therefore focus on the filling operation limited to $\mathcal{O}$. This can be done by considering any matrix generated from a word in the braid generators $\{\sigma_1, \sigma_2\}$. This $SU(2)$ element is in most cases outside $\mathcal{O}$; but it can be sent to $\mathcal{O}$ by the appropriate G element. Generically, each new word therefore brings a new element in $\mathcal{O}$. Figure 3 shows such ortoscheme filling for all words up to length 7. Applying the G group 14 400 elements (by concatenating braids on the left and the right with the known 120 Y elements) eventually leads to an already quite dense $SU(2)$ covering.

As an example, let us consider the $SU(2)$ matrix $\mathrm{i}\sigma_x$, which was approximated along a brute force search in [5, 6], where a braid of length 44 is found at a distance of about 10^{-3} of $\mathrm{i}\sigma_x$. Here a solution, equivalent under the G symmetry group, and with the same order of magnitude accuracy, can be found with a braid of half of this length, which then strongly reduces the brute force search. Note however that the full braid (with the G elements acting on the left and right) will eventually be longer than 44.

5. Conclusions and comments

Topological quantum computation with Fibonacci anyons strongly relies on the possibility of closely approaching any unitary matrix upon braiding the anyons. In this paper, we have shown how to fulfil this task for the 'three anyons–one qubit' case, by generalizing the standard geodesic dome covering of the sphere S^2 to the '$SU(2)$–S^3' hyperdome case. The efficiency of this construction is due to the close, and yet unexplored, relation between Fibonacci braid

generators and the binary icosahedral group generators. As a consequence, iterative finer and finer $SU(2)$ meshes can be generated, in a controlled way, with braid words of limited length.

Generalization to many qubits (with more Fibonacci anyons) is not easy. The first step would consist of selecting the high order discrete subgroup of $SU(N)$ and try to approach their generating set by braiding the anyons. As usual, one should first focus on one- and two-qubit gates, since it is known that generic $SU(N)$ can be generated by their suitable concatenation. So the natural next step will be to analyze the 'two-qubits $SU(4)$' case.

One way, presently still under study, is to first analyze nice discrete sets of two-qubits related by symmetry, and simply associated with successive shells of the eight-dimensional dense lattice $E8$ [13]. The first shell, with 240 points, corresponds (upon modding out a global phase factor) to 60 two-qubit 'physical' states: 36 product states and 24 maximally entangled (EPR) states. The product states are easily generated by separately braiding two sets of three braids (one needs only to use elements from the binary tetrahedral group, a Y subgroup). The entangled states will require more subtle braiding operations, such that they keep the system inside the two-qubit Hilbert space. Taking advantage of known properties about $E8$ shellings [14] (together with the entanglement sensitive S^7 Hopf fibration [15]), larger sets of two-qubit states with intermediate entanglement could also be generated.

Acknowledgments

It is a pleasure to acknowledge discussions with Pedro Ribeiro, Raphael Voituriez and David Bessis. This work (except the alternative method described in section 4) was presented at the Dublin workshop on topological quantum computing in September 2007, where I benefitted from remarks by D Bonesteels and M Freedman.

Appendix A. $SU(2)$ matrices, quaternions and the S^3 sphere

Quaternions are usually presented with the imaginary units $\mathbf{i}$, $\mathbf{j}$ and $\mathbf{k}$ in the form:

$$q = x_0 + x_1\mathbf{i} + x_2\mathbf{j} + x_3\mathbf{k}, \qquad x_0, x_1, x_2, x_3 \in \mathbb{R} \tag{A.1}$$

with $\mathbf{i}^2 = \mathbf{j}^2 = \mathbf{k}^2 = \mathbf{ijk} = -1$, the latter 'Hamilton' relations defining the non-commutative quaternion multiplication rule. The conjugate of a quaternion q is $\overline{q} = x_0 - x_1\mathbf{i} - x_2\mathbf{j} - x_3\mathbf{k}$ and its squared norm reads $N_q^2 = q\overline{q}$. The set of normed (or unit) quaternions will be denoted by Q.

Quaternions can also be defined equivalently, using the complex numbers $c_1 = x_0 + x_1\mathbf{i}$ and $c_2 = x_2 + x_3\mathbf{i}$, in the form $q = c_1 + c_2\mathbf{j}$, or equivalently as an ordered pair of complex numbers satisfying

$$(c_1, c_2) + (d_1, d_2) = (c_1 + d_1, c_2 + d_2) \tag{A.2}$$

$$(c_1, c_2)(d_1, d_2) = (c_1 d_1 - c_2\overline{d_2}, c_1 d_2 + c_2\overline{d_1}). \tag{A.3}$$

Generic $SU(2)$ matrices read

$$M = \begin{pmatrix} a + \mathbf{i}b & c + \mathbf{i}d \\ -c + \mathbf{i}d & a - \mathbf{i}b \end{pmatrix}, \qquad \text{with} \quad a^2 + b^2 + c^2 + d^2 = 1. \tag{A.4}$$

The latter relation (unit determinant) identifies $SU(2)$ with the three-dimensional sphere S^3. Writing M as

$$M = a\begin{pmatrix} 1 & 0 \\ 0 & 1 \end{pmatrix} + b\begin{pmatrix} \mathbf{i} & 0 \\ 0 & -\mathbf{i} \end{pmatrix} + c\begin{pmatrix} 0 & 1 \\ -1 & 0 \end{pmatrix} + d\begin{pmatrix} 0 & \mathbf{i} \\ \mathbf{i} & 0 \end{pmatrix} \tag{A.5}$$

allows us to write M as the unit quaternion

$$M = a + b\mathbf{i} + c\mathbf{j} + d\mathbf{k}, \tag{A.6}$$

with the identification

$$\mathbf{i} \equiv \begin{pmatrix} \mathbf{i} & 0 \\ 0 & -\mathbf{i} \end{pmatrix}, \qquad \mathbf{j} \equiv \begin{pmatrix} 0 & 1 \\ -1 & 0 \end{pmatrix}, \qquad \mathbf{k} \equiv \begin{pmatrix} 0 & \mathbf{i} \\ \mathbf{i} & 0 \end{pmatrix}. \tag{A.7}$$

Appendix B. Hopf map representation of $SU(2)$ matrices

A fibred space E is defined by a (many-to-one) map from E to the so-called 'base space', all points of a given fibre F being mapped onto a single base point. A fibration is said 'trivial' if the base B can be embedded in the fibred space E, the latter being faithfully described as the direct product of the base and the fibre (think, for instance, of fibrations of R^3 by parallel lines R and base R^2 or by parallel planes R^2 and base R).

The simplest, and most famous, example of a non-trivial fibration is the Hopf fibration [16] of S^3 by great circles S^1 and base space S^2. One standard notation for a fibred space is that of a map $E \xrightarrow{F} B$, which reads here $S^3 \xrightarrow{S^1} S^2$. Its non-trivial character implies $S^3 \neq S^2 \times S^1$.

To describe this fibration in an analytical form, we define elements of S^3 as pairs of complex numbers (α, β) which satisfy $|\alpha|^2 + |\beta|^2 = 1$.

The Hopf map is defined as the composition of a map h_1 from S^3 to $R^2(+\infty)$, followed by an inverse stereographic map h_2 from R^2 to S^2 :

$$\begin{array}{lccll} h_1\text{:} & S^3 & \longrightarrow & R^2 + \{\infty\} & \\ & (\alpha, \beta) & \longrightarrow & C = \alpha\beta^{-1} & \alpha, \beta \in \mathbb{C} \\ h_2\text{:} & R^2 + \{\infty\} & \longrightarrow & S^2 & \\ & C & \longrightarrow & M(X, Y, Z) & X^2 + Y^2 + Z^2 = 1 \end{array} \tag{B.1}$$

The first map h_1 clearly shows that the full S^3 great circle, parametrized by $(\alpha \exp(\mathrm{i}\omega), \beta \exp(\mathrm{i}\omega))$, is mapped onto the same single point with complex coordinate C. The Hopf map is therefore a means of representing $SU(2)$ matrices, either on the complex plane or on the sphere S^2, but with identical images for matrices differing only upon multiplication by the matrix

$$\begin{pmatrix} \exp(\mathrm{i}\omega) & 0 \\ 0 & \exp(-\mathrm{i}\omega) \end{pmatrix}. \tag{B.2}$$

Appendix C. Polytope {3, 3, 5}

Let us first recall the $\{p, q\}$ and $\{p, q, r\}$ Schläffli notations. $\{p, q\}$ denotes a regular two-dimensional tiling (either spherical, Euclidean or hyperbolic), such that each site belongs to q regular p-gones: $\{4, 3\}$ is a cube, $\{6, 3\}$ is a honeycomb tiling. $\{p, q, r\}$ is a regular three-dimensional tiling, such that each edge belongs to r polyhedra of the type $\{p, q\}$: $\{4, 3, 4\}$ is the standard cubic tiling in R^3.

So, $\{3, 3, 5\}$ denotes a tiling of regular tetrahedra $\{3, 3\}$, with exactly five such tetrahedra sharing an edge. The regular tetrahedron dihedral angle being slightly less than $2\pi/5$, this

leads to a polytope structure on the three-dimensional curved space S^3 (embedded in R^4) [9, 10]. It contains:

- 120 vertices,
- 720 edges,
- 1200 triangular faces,
- 600 tetrahedral cells.

Note that these numbers satisfy the (S^3) generalized Euler–Poincaré relation,

$$V - E + F - C = 0 \tag{C.1}$$

where V, E, F, C are (respectively) the number of vertices, edges, faces and cells.

With one vertex on the pole, the successive 'horizontal' sections are (i) an icosahedral shell, (ii) a dodecahedral shell, (iii) a new icosahedral shell and (iv) an equatorial icosidodecahedral shell. The next shells then symmetrically reproduce the same pattern down to the S^3 south pole.

The dual polytope $\{5, 3, 3\}$ has 600 vertices and 120 dodecahedral cells.

The $\{3, 3, 5\}$ symmetry group plays an important role in the present study. S^3 orientation preserving point symmetries forms the group $SO(4)$, while the full group is $O(4)$. Symmetry elements are easily written in terms of unit quaternions. For the $SO(4)$ action, a given point on S^3, labelled by the quaternion q, is sent to lqr, with $l, r \in Q$ (with an additional quotient by Z_2, see below). The remaining indirect symmetries in $O(4)$ are such that q is sent to $l\bar{q}r$.

The (properly oriented) $\{3, 3, 5\}$ 120 vertices (on a unit radius S^3) are in one-to-one correspondance with the 120 elements of the binary icosahedral group Y. Due to the group structure, multiplying on the left or the right by Y elements sends the polytope onto itself. Recalling that the group centre is just $\{1, -1\}$, one finds as a whole the 7200 elements of the orientation preserving group G' (discrete subgroup of $SO(4)$).

$$G' = Y \times Y / Z_2. \tag{C.2}$$

The full group G includes 7200 additional indirect transformations, which read

$$q \to l\bar{q}r \qquad l, r \in Y, \tag{C.3}$$

leading as a whole to the G 14 400 elements.

This order can also be computed directly from the number of fundamental regions; for a regular polytope, this amounts to generating the tetrahedral orthoscheme $\mathcal{O}$ associated with the full symmetry group, such that the latter is generated by reflections about the orthoscheme faces. One orthoscheme is simply built from a regular cell $\{p, q\}$ of the $\{p, q, r\}$, by selecting a cell vertex V, a middle edge point E (for an edge through the selected vertex), a middle face point F (for a face sharing the cell vertex and the selected edge) and finally the cell centre C (see figure D2(left))

Polytope $\{3, 3, 5\}$ has 600 tetrahedral cells. Each cell being decomposed into 24 orthoschemes, one recovers the 14 400 fundamental regions and therefore the G group order. If one lets the G generators freely act onto a point M in one orthoscheme $\mathcal{O}$, one eventually gets a set $\mathcal{P}$ of N regularly spaced points on S^3, with N depending on the location of M:

- If M coincides with V, $N = 120$ and $\mathcal{P}$ is a $\{3, 3, 5\}$ polytope;
- If M coincides with C, $N = 600$ and $\mathcal{P}$ is a $\{5, 3, 3\}$ polytope;
- If M is a generic point on a $\{3, 3, 5\}$ edge, $N = 1440$, while $N = 720$ if M at a mid-edge position;
- For a generic M inside $\mathcal{O}$, the number of images is maximal, $N = 14\,400$.

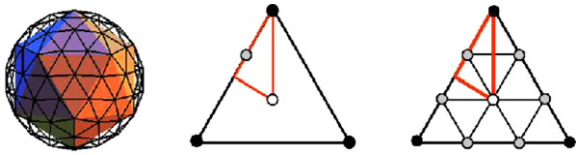

Figure D1. Left: geodesic dome based on icosahedral symmetry; centre: an icosahedron triangular cell, with a (fundamental region) orthoscheme decorated with three vertices (the so-called seed set $\mathcal{S}$): a triangular cell vertex V (black circle), a face centre F (white circle), a vertex D at one third on an edge(grey circle). Right: triangle cell decoration obtained as the local images of the three points in the orthoscheme.

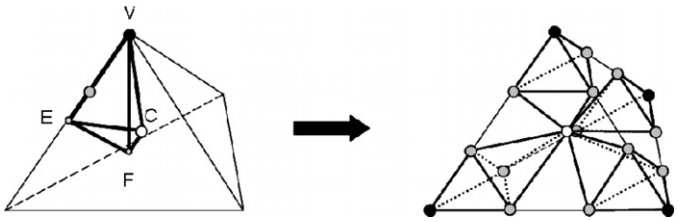

Figure D2. Left: a tetrahedral $\{3, 3, 5\}$ cell, with one fundamental orthoscheme whose four vertices are a cell vertex V, a mid-edge point E, a face centre F and the cell centre C. The figure also shows the decoration of the orthoscheme by the seed set $\mathcal{S}_1^{\mathcal{P}}$, with V (black circle), C (white circle), and a third point located at one third on an edge (grey circle). Right: the cell decoration for $\mathcal{P}_1$, obtained as the local images of $\mathcal{S}_1^{\mathcal{P}}$.

Finally, as discussed in the text (and in the next appendix), one also considers sets $\mathcal{P}$ which are the image under G of several points M, forming a seed set $\mathcal{S}$.

Appendix D. Geodesic hyperdomes

Geodesic domes are triangulations of the sphere S^2, usually built with icoshaedral symmetry. There are several different families of such discrete sets, the simplest being obtained by the decomposition of icosahedron triangular faces into smaller triangles. Figure D1 (left) shows an example with 92 vertices, where edges are scaled by a factor three (this factor is only approximate if the dome vertices and edges are centrally mapped onto the sphere S^2). The geodesic dome shares the same symmetry group as the original icosahedron. Its vertices can therefore be generated from a seed set $\mathcal{S}$ located in one of the group orthoschemes. Figure D1 (centre) displays such an orthoscheme, inside a triangular face, with $\mathcal{S}$ made of three points, a face vertex V, face centre F and a point D at one third along an edge. The seed set is then propagated under the group action, here a reflection in the orthoscheme edges, leading to the geodesic dome 92 vertices in the following way: V has 12 images (forming the original icosahedron), F has 20 images (forming the dual dodecahedron) and D has 60 images (forming a 'buckyball' polyhedron). Figure D1 (right) shows the image of $\mathcal{S}$ propagated inside one triangle of the original icosahedron.

The generalization to S^3 proceeds along similar lines. Take a $\{3, 3, 5\}$ tetrahedral cell (figure D2 (left)), with one orhoscheme and the three seed vertices described in section 3.2. And then propagate the seed set under the G group action. Figure D2 (right) shows the image of the propagated seed set, restricted to a $\{3, 3, 5\}$ tetrahedral cell.

References

[1] Kitaev A Y 2003 *Ann. Phys.* **303** 2
[2] Freedman M H, Larsen M J and Wang Z 2002 *Commun. Math. Phys.* **227** 605
[3] Lecture notes for physics 219: quantum computation, available at http://www.theory.caltech.edu/preskill
[4] Sarma S D, Freedman M, Nayak C, Simon S H and Stern A 2007 Non-Abelian anyons and topological quantum computation (*Preprint* 0707.1889)
[5] Bonesteel N E, Hormozi L, Zikos G and Simon S H 2005 *Phys. Rev. Lett.* **95** 140503
[6] Hormozi L, Zikos G, Bonesteel N E and Simon S H 2007 *Phys. Rev.* B **75** 165310
[7] Kitaev A Y, Shen A H and Vyalyi M N 1999 *Classical and Quantum Computation* (Providence, RI: American Mathematical Society)
[8] Nielsen M A and Chuang I L 2000 *Quantum Computation and Quantum Information* (Cambridge: Cambridge University Press)
[9] Coxeter H S M 1973 *Regular Polytopes* (New York: Dover)
[10] Sadoc J-F and Mosseri R 1999 *Geometrical Frustration* (Cambridge: Cambridge University Press)
[11] Mosseri R and Sadoc J-F 1984 *J. Phys. Lett.* **45** L827–32
[12] Sadoc J-F and Mosseri R 1985 *J. Phys.* **46** 1809–26
[13] Rigetti C, Mosseri R and Devoret M 2004 *Quantum Information Processing* vol 3 (Berlin: Springer) pp 351–80
[14] Sadoc J-F and Mosseri R 1993 *J. Phys. A: Math. Gen.* **26** 1789
[15] Mosseri R and Dandoloff R 2001 *J. Phys. A: Math. Gen.* **34** 10243–52
[16] Hopf H 1931 *Math. Ann.* **104** 637–65